Analysis of 4D CT cine images for the characterization of organ motion due to breathing

Maria Francesca Spadea[1,2], Marta Peroni[2], Marco Riboldi[2], Guido Baroni[2], George TY Chen[3], Gregory Sharp[3]

1 Department of Experimental and Clinical Medicine, University of Magna Graecia, Catanzaro, Italy, 2 Bioengineering Department, Politecnico di Milano University, Milano, Italy, 3 Massachusetts General Hospital – Harvard Medical School, Boston, MA, USA

Abstract. A semi-automatic procedure to correlate the motion of lung tumor points in 4D-CT images with a respiratory surrogate signal is presented. Data analysis was performed to characterize of the robustness of external/internal correlation properties in the clinical framework of gated radiotherapy treatments. A cross-correlation based algorithm was implemented to perform template matching for tracking the spatial movement of tumor's points in 6 patients. A graphical interface was developed to allow users to navigate through un-binned CT images. The detected internal movement of features in 3D was then retrospectively synchronized with the RPM signal, and the correlation index R^2 was computed. Results also include the range of motion of selected points, and the prediction error. The developed procedure allowed a fast analysis for external/internal correlation of lung anatomy. The study is generally relevant for all the treatments in which organ motion compensation and control is an issue.

Keywords: organ motion, 4D-CT, lung tumor, external/internal correlation.

1 Introduction

Organ motion due to breathing is an issue in different medical treatments such as radiotherapy [1], [2] and robotic assisted surgery [3], [4], where the main goal is to improve the accuracy of therapeutic procedures while being minimally invasive. Problems occur at different levels: first of all, image artifacts on diagnostic images do not provide consistent information for treatment planning; secondly, the know how transfer from treatment plan to intra-operative environment can be not obvious if the treated position and the expected position of an internal target differ.

For instance, in the radiation therapy framework, the actual delivered dose to the patient might diverge from the planned dose because of anatomical changes during the beam delivery in a treatment fraction (intra-fraction) or in between fractions (inter-fraction), as compared to the time of treatment planning.

Recently, conventional radiotherapy and surgery have moved in the direction of Image Guided Radiotherapy (IGRT) [5] and Image Guided Surgery (IGS) [6], for which on-line tools have been developed by many companies to follow the moving organs during a treatment and from one fraction to the next one. Time-resolved imaging techniques, such as 4-Dimensional Computer Tomography (4D-CT), are increasingly emerging as optimal strategy to overcome motion artifacts and limitations in diagnostic imaging and treatment planning/delivering (4D imaging, 4D treatment planning, 4D dosimetry). In this imaging modality, multiple images are acquired during the respiratory cycle and retrospectively sorted into volumetric image sets corresponding to different breathing phases. A respiratory signal (usually the motion of external surface) must also be acquired and synchronized with the image formation process. Hence, 4D data can be analyzed to determine the mean tumor position, tumor range of motion for treatment planning, the relation of tumor trajectory to other organs and to extend the static treatment plan to the all phases of the respiration cycle. However, a limitation of 4D CT is that it is affected by variations in respiratory patterns during acquisition. A second issue arises in the correlation between external fiducial movement and tumor/organ motion. The relation of between the motion of internal and external anatomy need to be assed to exploit the benefits of both IGRT and IGS techniques.

This work follows a previous pilot study [7], aiming at assessing the correlation between the motion of external fiducials and internal features in lung tumors on the basis of 4-Dimensional Computer Tomography (4D-CT) data. Previously, vessel bifurcations were selected as inner targets to be correlated with RPM signal. In this case, the motion of tumor points were tracked. Data analysis was conducted to extract the Spearman correlation coefficient, the range of motion of the tumor, the prediction error in tracking the internal motion from the external fiducial monitoring.

2 Material and Methods

The 4DT-CT data of a group of 6 lung patients (pt) were used in this study. Images were acquired through a 4-slice scanner (LightSpeed QX/i, GE Medical Systems, Milwaukee, WI) operating in axial cine-mode. Patients' breathing signal was provided by the Real-Time Position Management system (RPM, Varian® Medical System, Palo Alto CA), in which a single surface surrogate (infra-red marker block) is tracked in real-time with a video camera positioned at the foot of the CT couch [8]. The RPM block was placed abdominal surface of the patient. According to protocol in use at our Institute, described in detail in Rietzel *et al* [8], a pre-determined number N of 4-slice chunks (Ch_i with i=1…N) was acquired at each couch position (CP). Images were reconstructed from 360° projections, which require either 0.8 or 1.0 seconds to acquire (T_r). For analysis purposes, we assume the acquisition occurs instantaneously at the mid-scan time, half way through the full rotation. The CP time duration (cine duration, T_{cine}) was set on the basis of the observed subject's breathing period plus the time required for a tube rotation. Therefore, the number N varied among patients as a function of the T_{cine}, T_r and of the midscan time delay (ΔMidscan time) between 2 contiguous images in a CP, according to the following equation :

$$N = \frac{(T_{cine} - T_r)}{\Delta Midscan} + 1 \quad \textbf{(1)}$$

The acquisition of projections at each CP starts independently of the current respiratory state and therefore no correspondence exists between Ch_i at different couch positions. At each couch position, the coverage in superior-inferior (SI) direction was 1 cm (2.5 mm thickness per 4 slices). The resolution both in latero-lateral (LL) and anterior-posterior (AP) directions ranged from 0.76 mm to 0.98 mm.

2.2 Images processing: automatic feature matching algorithm

The time stamp of each image (midscan time) was time synchronized with the respiratory signal acquired by RPM system. Un-binned images were processed and sorted on the basis of acquisition time, and matched with the RPM. Anatomical landmarks in the lungs were selected in 4D-CT cine-data, and correlated with the respiratory signal.

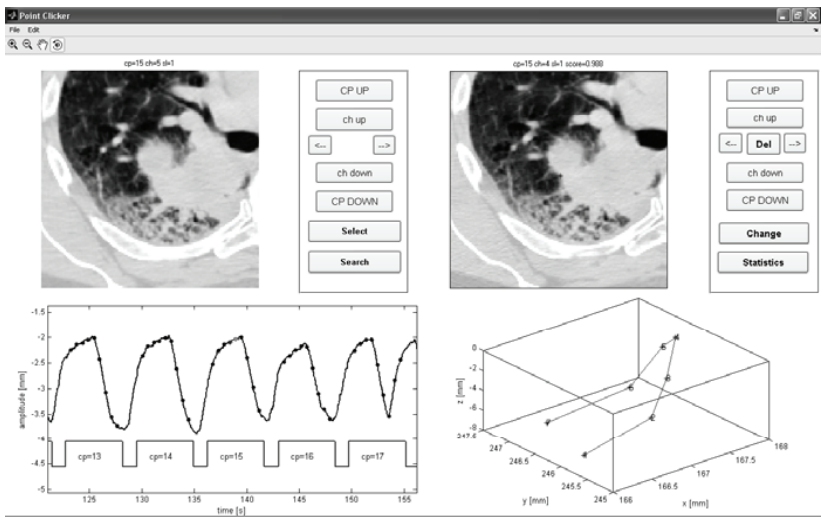

Fig. 1. View of the graphical user interface of the application. Upper left quarter, navigation panel and image for point selection. In the bottom left quarter, RPM trace with indication of the instant of time of the selected point keeps track of the position of the automatic searched point while navigating in the volume. Upper right quarter, navigation panel and image for verification of the semi-automatic procedure. In the bottom right quarter, 3D trajectory of the tracked point is updated in real-time according to navigation throughout the volume and user manual corrections.

A semi-automatic procedure for inner feature tracking in 4D-CT was developed in Matlab environment (MatLab® version 7.0, the MathWorks, Natick, MA). The user first chooses a point on a selected image (reference image) and then decides which

slices to include in the tracking process. A graphical interface assists the user in navigation within the 4D-CT volume data (see Fig. 1).

Through a virtual navigation keyboard one can select the CP, the Ch_i, and the slice within the couch position (sl_i with i=1…4, indicated above the panel). The selected point is marked with a green dot on the image, and its corresponding external position within the RPM respiratory trace is shown below, thus helping the user in choosing the couch positions to be included in the feature searching. This is shown on the left of Fig. 1, where a point is selected on the third slice of a 4-slice set acquired at the maximum inhale condition, and the green dot in the RPM plot below shows the external amplitude. The recommended automatic search region would therefore consist of the two previous couch positions plus the current one, since it is expected that the diaphragm will move superiorly. Feature tracking was based on a 2-D template matching image process. The template was defined as a matrix of 62x62 pixels centered in the point selected on the reference slice. The cross-correlation matrix between the template and the searching window (92x92 pixels) was computed for each slice encompassed in the selected volume. The pixel location (in terms of row and column indexes of the image searching window) in each processed image corresponding to the maximum value of the correlation coefficient (score) was selected as result of the template matching. Hence, a correlation score (ranging from 0 to 1) was obtained for each slice at every respiratory phase in correspondence of the three couch positions. A second image (on the right in figure 2) is produced for the verification of the semi-automatic procedure, which is again assisted by interactive navigation. For each chunk the slice with maximum score (among the 4 ones) is presented. The user may accept the result, change the location of the feature position along the LL and AP directions and/or within the 4 slices or delete the selected feature if it is not present. The 3D trajectory of the point is showed below the verification CT slice. To increase the resolution along the superior-inferior (SI) direction, a 2^{nd}-order spline, interpolating the best score values in the 4 slices of each phase, was computed. An example of the interpolation procedure is showed in Fig. 2. Feature SI-location was selected according to the maximum of the interpolant function.

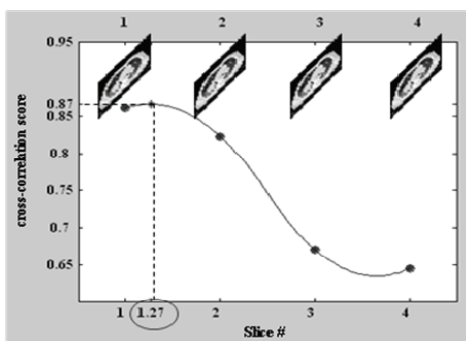

Fig. 2. Example of spline interpolation between slices. In this case scores were 0.864, 0.829, 0.675, 0.650 for slice 1, 2, 3, 4 respectively. Maximum value of the interpolant was found between slices 1 and 2

2.3 Data analysis

For each patient 3 points (each one in a different couch positions, from head to feet) on the edge of the cancer mass were tracked. The detected internal movement of tumor's points was correlated with the RPM signal and analyzed for linear correlation. A dedicated section in the algorithm was implemented to analyze data in terms of the motion amplitude and the correlation index R2 of the linear fitting over the entire patient population. In order to measure the prediction error of the internal motion based on the external signal, a cross validation leave-one-out was implemented. This analysis was enriched by a 3-dimentional linear fitting to understand if a 2 parameter model based on external motion amplitude and its gradient can better fit the internal movement (see Fig. 3).

The results were supported by non parametric statistical analysis computed by means of the software Statistica 6.0 (StatSoft Inc, Tulsa OK, USA).

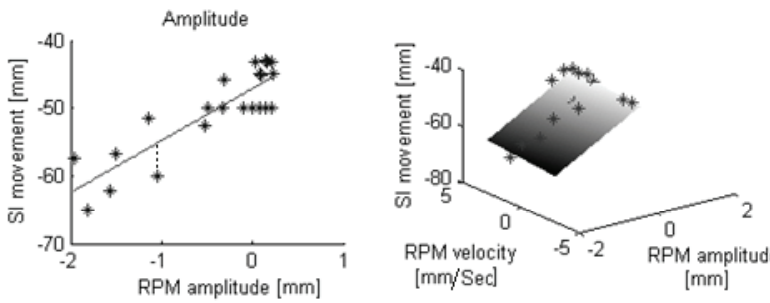

Fig. 3. Example of the line and plane fitting to extract internal external correlation.

4 Results

In Figure 4, the correlation index R^2 between the external and the internal motion in each direction is shown (p-value<0.01). Maximum values of R^2 (95% of confidence interval) are in SI direction, being the median±quartile 0.93±0.09 . Internal motion along LL and AP direction featured low correlation with the movement of the external point (0.51±0.52 and 0.66±0.32 in LL and AP respectively).

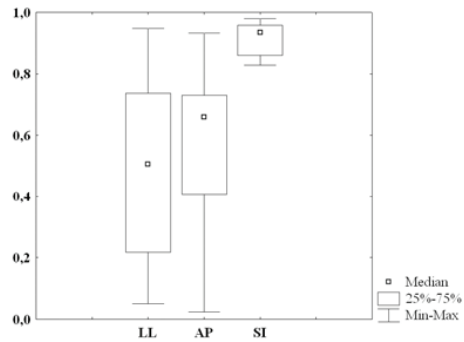

Fig. 4. Median±quartile and min-max range of R2 in each direction.

Statistical difference between R2-SI and R2-LL/AP was proved through Kruskall-Wallis test. In table 1, the range of motion averaged on the set of three selected points for each subject is presented. Patient 3 exhibited largest tumor motion in AP and SI directions, being up to 8 mm and 17 mm respectively. LL direction was most stable except for Patient 2 (up to 6 mm about).

Table 1. Estimated range of motion of the tumor obtained through the analysis of the movement of 3 points. Mean (standard deviation) values over three points are reported.

Patient #	LL (mm)	AP (mm)	SI (mm)
P1	1.94 (0.22)	2.21 (0.98)	6,08 (1.33)
P2	5.45 (0.85)	2.16 (1.12)	8,17 (2.37)
P3	2.67 (0.79)	7.16 (0.69)	16,28 (0.62)
P4	1.16 (0.58)	0.71 (0.38)	8,31 (1.40)
P5	0.26 (0.23)	3.32 (0.52)	6,05 (1.18)
P6	0.91 (0.49)	3.26 (1.13)	6,54 (1.73)

In a effort to understand repeatability of tumor motion over different breathing cycles, we compared the trajectory of the three points of the tumor. Patient 3 is reported in Fig. 5 as an example: in this case, the three points were tracked on couch position number 15, 16 an 18.

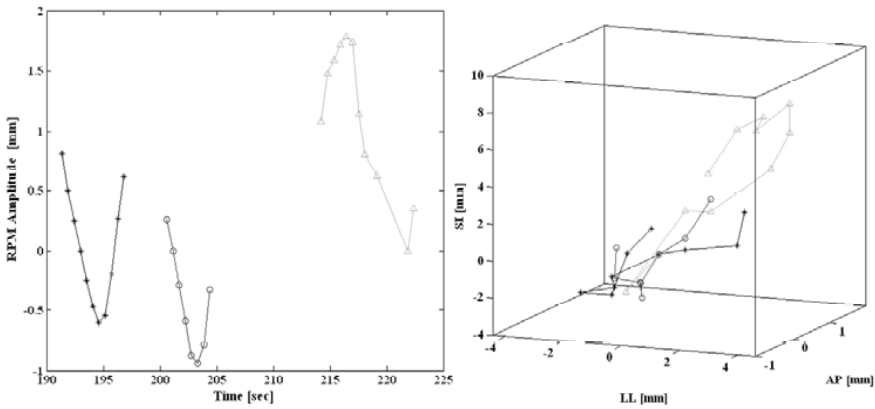

Fig. 5. Trajectory of three points selected at the beginning (*), middle (○) and towards the end (⅄) of the lesion of Patient 3.

Points 1 and point 2 were visible only in few phases for the selected respiration cycle, as is observable in the left panel of the figure. Extensions over contiguous CP were not considered in this analisys Qualitative examination demonstrates a quite good repeatability of the trajectory of points belonging to the same anatomical structure in different breathings, especially in the SI direction.

Considering the prediction error, the RPM amplitude-based (2D) prediction was compared to the RPM amplitude and velocity-based prediction (3D) and results are reported in table 2. Wilcoxon matched pair test revealed no statistical difference between the two methods. Maximum values were found in SI direction of Patient 3 (about 2 mm).

Table 2. RPM amplitude-based (2D) prediction and RPM amplitude and velocity-based prediction (3D)

	Prediction Error 2D			**Prediction Error 3D**		
	LL (mm)	AP (mm)	SI (mm)	LL (mm)	AP (mm)	SI (mm)
25%	0,26	0,30	0,50	0,25	0,29	0,43
Median	0,34	0,48	0,74	0,31	0,43	0,60
75%	0,37	0,73	1,14	0,34	0,69	1,03

We put forward the hypothesis that there is a relation between the size of the prediction error and the size of the range of motion. This is supported by results displayed in Fig. 6 (2D prediction error vs. range of motion). Although a good linear relation cannot be demonstrated, the increasing trend of prediction error as a function range of motion is evident (p value<0.001).

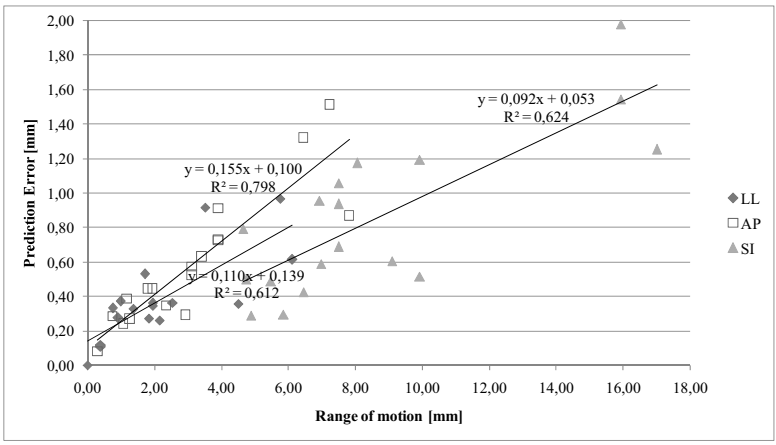

Fig. 6. Analysis of the relation between range of motion and prediction error.

Discussion and Conclusion

In this work, we present a semi-automatic and fast method for characterizing the correlation between the external surface movement and internal tumor motion using the same data and images that are routinely acquired for 4D-CT. Most of literature about this topic in the radiotherapy field is based on data acquired by using fluoroscopic imaging [9], [10], [11]. Although these studies sufficiently describe the tumor motion and the quality of external/internal correlation, they are not based on a protocol widely spread into the clinical practice. Furthermore, the monitoring of internal movements by using fluoroscopic images requires the implantation of seeds, which represents a serious hazard for lung patients. Instead, 4D-CT based planning and treatment procedures are currently well-accepted, and RPM is the most widespread device used as surrogate of the breathing signal. For this reason it is crucial to understand the sensitivity of this instrument, and to evaluate how well it can estimate internal organ motion. The advantages of using cine-mode protocol, especially for investigations purposes, are widely described [8]. Because this analysis is based on the synchronization of cine mode images with the respiratory signal, no inaccuracies in phase detection and binning were introduced.

Our results revealed a good correlation between the internal SI motion and the external respiratory surrogate. Low correlation in the other directions is probably due to small range of motion in LL and AP. The size of range of motion also influence the size of the prediction error as shown in Fig. 6. However, the maximum value was about 2 mm that might be considered acceptable as extreme limit for gated radiotherapy.

In conclusion, we have developed a automatic procedure and analysis tools for studying the correlation between the internal and external motion in lung tumors, using data already routinely acquired for 4D-CT. This tool will aid in predicting internal motion through external surrogates. Further research is needed to improve the accuracy and spatial coherence of internal anatomy in 4D CT data acquisition

References

1. Goitein, M. Organ and tumor motion: an overview. Semin. Radiat. Oncol. 14(1), 2-9 (2004)
2. Keall, P.J., Mageras, G.S., Balter, J.M. et al. The management of respiratory motion in radiation oncology report of AAPM Task Group 76. Med. Phys. 33(10),
3. Müller, S.A., Maier-Hein, L., Mehrabi, A., et al. Creation and establishment of a respiratory liver motion simulator for liver interventions. Conf. Proc. IEEE Eng. Med. Biol. Soc. 2614-2617 (2007)
4. Lesniak, J., Tokuda, J., Kikinis, R., Burghart, C., Hata, N. A device guidance method for organ motion compensation in MRI-guided therapy. Phys. Med. Biol. 52(21), 6427-6438 (2007)
5. Xing L, Thorndyke B, Schreibmann E, Yang Y, Li TF, Kim GY, Luxton G, Koong A. Overview of image-guided radiation therapy. Med. Dosim. 31(2):91-112 (2006).
6. Marescaux, J., Solerc, L. Image-guided robotic surgery. Semin Laparosc Surg. 11(2), 113-122 (2004)
7. Spadea, M.F., Riboldi, M., Baroni, G., Chen, G.T.Y., Sharp, G. A Feature matching approach for the automatic correlation of internal and external motion in lung tumors. Med. Phys. 34 (Suppl. 1): 2390-2391 (2007)
8. Rietzel E, Pan T, Chen CTY. Four-dimensional computed tomography: Image formation and clinical protocol. Med. Phys. 32(4), 874-888 (2005)
9. Gierga, D.P., Brewer, J., Sharp, G.C., Betke, M., Willett, C.G., Chen, G.T. The correlation between internal and external markers for abdominal tumors: implications for respiratory gating. Int J Radiat Oncol Biol Phys. 61(5), 1551-1558 (2005)
10. Hoisak, J.D.P., Sixel, K.E., Tirona, R., Cheung, P.C.F., Pignol, J.P. Correlation of lung tumor motion with external surrogate indicators of respiration. Int J Radiat. Oncol. Biol. Phys., 60(4):1298:1306 (2004).
11. Yan H, Yin FF, Zhu GP, Ajlouni M, Kim JH. The correlation evaluation of a tumor tracking system using multiple external markers. Med Phys. 2006 Nov;33(11):4073-4084.